water

MDPI

Article

Physical Modeling of Seepage Control Using Upstream Blanket and Cutoff in Earth Dams: A Hele–Shaw Experimental Study

Ahmed M. Abdelrazek [1,2,*], Mohamed A. Hafez [2,3], Abdulrahman Mohammed [1] and Mohammed A. Abourohiem [2]

[1] Department of Engineering Management, College of Engineering, Prince Sultan University, Riyadh 11586, Saudi Arabia; 221211508@psu.edu.sa
[2] Irrigation Engineering and Hydraulics Department, Faculty of Engineering, Alexandria University, Alexandria 21544, Egypt; hafezm2@mcmaster.ca (M.A.H.); mrohiem76@yahoo.com (M.A.A.)
[3] Civil Engineering Department, Faculty of Engineering, McMaster University, Hamilton, ON L8S 4L7, Canada
* Correspondence: aibrahim@psu.edu.sa; Tel.: +966-5363-09852

Abstract

Seepage beneath earth dams founded on pervious strata can cause excessive under-seepage, elevated downstream exit gradients, and high phreatic levels, thereby increasing susceptibility to internal erosion and piping. This study presents a Hele–Shaw laboratory investigation of seepage-control efficiency for an upstream impervious blanket used alone and in combination with a vertical cutoff (blanket–cutoff system). The experimental geometry reproduces a zoned earth dam cross-section at a scale of 1:200. Five foundation thickness ratios ($T/B = 0.184$–1.00) were tested. For the blanket-only system, four blanket length ratios ($L_b/B = 0.50$–1.25) were examined. For the blanket–cutoff system, cutoff depth ratios ($S/T = 0.20$–0.80) were investigated using (i) a representative blanket length $L_b/B = 0.75$ across all foundation depths and (ii) a deep-foundation case $T/B = 1.00$ across all blanket lengths. Seepage discharge, head loss due to seepage-control measures, maximum exit gradient at the downstream toe, and phreatic line location were measured at steady state and expressed in dimensionless form using the equivalent Hele–Shaw hydraulic conductivity. Relative to the no-measure reference case, the upstream blanket reduced dimensionless discharge by 20.8–70.2%, reduced the exit-gradient indicator by 6.4–50.2%, and reduced the downstream seepage-surface height by 58.9–92.8%. Adding a vertical cutoff provided further reductions relative to the blanket-only configuration, up to 34.4% in discharge and to 29.8% in exit-gradient indicator at $L_b/B = 0.75$—while increasing head loss across the upstream control system. Regression-based correlations and main-text design maps are proposed for preliminary sizing. The proposed correlations and design maps are intended for screening-level use only within the tested ranges $0.18 \leq T/B \leq 1.00$, $0.50 \leq L_b/B \leq 1.25$, and $0.20 \leq S/T \leq 0.80$. Because the Hele–Shaw model is a two-dimensional viscous-flow analog of saturated seepage, the results provide a physical basis for relative comparison of seepage-control measures rather than a direct substitute for site-specific analysis of heterogeneous three-dimensional foundations. Accordingly, the agreement discussed in this paper is qualitative and trend-based, and the proposed tools are intended to complement rather than replace quantitative FEM for site-specific design.

Keywords: seepage flow; earth dams; hydraulic gradient; piping risk; upstream blanket; cutoff wall; Hele–Shaw model; hydraulic modeling

Check for updates

Academic Editors: Hossein Kheirkhah Gildeh, Majid Mohammadian and Xiaohui Yan

Received: 11 March 2026
Revised: 16 April 2026
Accepted: 18 April 2026
Published: 21 April 2026

Copyright: © 2026 by the authors. Licensee MDPI, Basel, Switzerland. This article is an open access article distributed under the terms and conditions of the Creative Commons Attribution (CC BY) license.

1. Introduction

Seepage is a primary serviceability and safety concern in embankment (earth) dams, influencing leakage losses, uplift pressures, slope stability, and, critically, the potential for internal erosion and piping. Contemporary practice emphasizes integrated approaches across seepage control, detection, and treatment, with solutions tailored to site-specific geology and operational constraints [1].

Internal erosion and piping are strongly linked to hydraulic gradients and seepage-induced stress conditions, particularly at the downstream toe, where exit gradients may become critical [2]. Laboratory evidence also indicates that cyclic or varying hydraulic gradients can accelerate erosion mechanisms in gap-graded cohesionless materials, highlighting the importance of controlling both steady-state and evolving seepage regimes [3].

Seepage mitigation commonly relies on cutoff walls or sheet piles, upstream impervious blankets, filters/drains, or combinations thereof. Recent research continues to explore combined measures (e.g., cutoff walls + horizontal drainage), showing notable reductions in seepage-related risks and often identifying diminishing returns beyond certain geometric thresholds [4,5]. Complementary strategies, such as drain pipes, can also reduce exit gradients and seepage flow while improving slope stability indices in numerical investigations [6]. Similarly, studies of sheet pile arrangements demonstrate measurable impacts on seepage characteristics and phreatic profiles, reinforcing the value of seepage-path modification and head-dissipation mechanisms [7].

From the study of seepage theory, an upstream blanket acts by increasing the horizontal distance over which hydraulic head is dissipated, thereby lowering the average gradient by acting beneath the upstream part of the foundation. A vertical cutoff alters the flow net more abruptly by forcing seepage beneath the cutoff tip, increasing the effective seepage path and shifting a larger share of the total potential drop upstream of the downstream toe. These mechanisms are consistent with Darcy-type seepage theory, but experimental datasets that simultaneously track discharge, head-loss redistribution, toe-gradient response, and phreatic-surface location for blanket–cutoff combinations remain limited.

Alongside deterministic studies, probabilistic and reliability-based seepage assessment has gained momentum to account for uncertainty and spatial variability in permeability [8,9], and transient seepage–stability coupling is increasingly recognized as important for realistic dam operation [10]. Durability of anti-seepage systems, especially cutoff walls, is also receiving attention through coupled seepage–dissolution modeling [11]. Additionally, data-driven models have been proposed to accelerate prediction and optimization of cutoff-wall performance [12].

Recent geotechnical studies also underscore that seepage problems may interact with nonlinear hydro-mechanical coupling and uncertainty. Cao et al. [13] developed a nonlinear seepage-mechanical model for fluid–solid coupling in fractured rock masses, while Zhu et al. [14] used random finite elements to show how stratification and spatial variability influence the probabilistic stability of two-layer undrained slopes. Although these studies address different geotechnical systems, they reinforce the broader need to interpret seepage control within a mechanistic and uncertainty-aware framework when translating laboratory observations to field design.

Analytical solutions for blankets and related seepage-control layouts remain useful for preliminary sizing and conceptual design [15–18]. However, the available literature is still dominated by analytical and numerical treatments, whereas experimental datasets that simultaneously quantify discharge, toe exit-gradient indicators, head-loss redistribution, and phreatic-line response for blanket–cutoff systems remain limited. Such physically measured data are needed both to assess piping-related hydraulic indicators and to support preliminary sizing of seepage-control measures in hydraulic structures.

The present manuscript is scientifically distinct from our 2021 conference paper [19]. The conference paper presented an analytical formulation for seepage through a deep pervious foundation with an upstream impervious blanket and vertical cutoff under idealized assumptions. In contrast, the present study provides a comprehensive Hele–Shaw experimental investigation of seepage control in earth dams founded on pervious foundations. The added scientific value is not merely a change in method from analysis to experiment; it is the direct measurement of the incremental hydraulic benefit of adding a cutoff to a blanket across a matrix of T/B, L_b/B, and S/T, together with physically observed phreatic-surface response and regression-based screening tools.

Relative to existing finite element modeling (FEM)-based seepage studies, the contribution here is not a one-to-one quantitative reproduction of a particular prototype, constitutive model, or boundary-value problem. Rather, the Hele–Shaw experiments provide a physically measured parametric dataset under controlled conditions, allowing direct observation of head-loss redistribution, phreatic-surface response, and toe-gradient trends. Relative to prior experimental studies, the distinction is the systematic combined evaluation of blanket-only and blanket–cutoff configurations across coupled ranges of T/B, L_b/B, and S/T using a common set of hydraulic response metrics.

Accordingly, the novelty of the present study lies in three points: (i) providing a physically measured dataset for blanket-only and blanket–cutoff seepage control over wide ranges of T/B, L_b/B, and S/T; (ii) directly quantifying exit-gradient indicators relevant to piping sensitivity; and (iii) developing compact design tools, including regression equations and design maps, for preliminary screening. The objectives of this work are to quantify the influence of foundation thickness ratio T/B, blanket length ratio L_b/B, and cutoff depth ratio S/T on normalized seepage discharge $q/(K_f H)$, head-loss ratio $\Delta H/H$, exit-gradient indicator $I_{ex,\max}(B/H)$, and phreatic-surface response, and to translate the results into screening-level design guidance for upstream blanket and blanket–cutoff systems. The novelty is therefore not the use of physical modeling alone, but the unified experimental quantification of coupled design variables and response indicators that can be used to screen layouts before detailed numerical analysis.

2. Materials and Methods

2.1. Prototype Case Study and Scaled Model Geometry

The experimental geometry was based on the Shiwashok zoned earth dam in the Kurdistan region of Iraq, as reported by Noori et al. [20]. The prototype dam geometry, as illustrated in Figure 1, is 23 m high (H_d), with a crest width (b) of 7 m, base width (B) of 136 m, and upstream head (H) of 20 m. It includes a 2 m berm on both embankment faces; the upstream slope is 1 V:2.75 H, whereas the downstream slope is 1 V:2.5 H above the berm and 1 V:2.75 H below it.

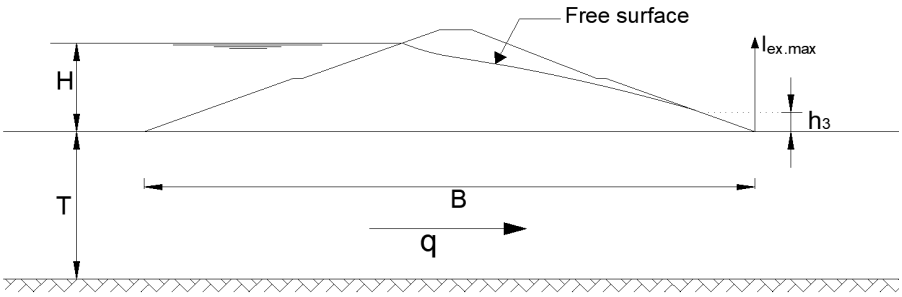

Figure 1. Prototype Shiwashok dam geometry (after [20]).

A geometric scale of 1:200 was adopted for the Hele–Shaw model, giving $H_d = 11.5$ cm, $b = 3.5$ cm, $B = 68$ cm, and $H = 10$ cm; the berm width in the model is 1 cm. The dam cross-section, including slopes and berm, was shaped on the front Perspex plate. Because the prototype dam is zoned and contains an impervious core, the dam body was treated in the present under-seepage-focused analog as an impervious boundary; thus, seepage was dominated by foundation flow beneath the dam and around the seepage-control elements.

2.2. Hele–Shaw Seepage Analogy and Equivalent Hydraulic Conductivity

A Hele–Shaw model consists of two closely spaced parallel plates. When the interspace is sufficiently small (typically 1.65 mm), viscous flow remains laminar, and the depth-averaged velocity is proportional to the hydraulic gradient, producing a Darcy-type analog behavior for seepage studies [21,22].

The viscous resistance between plates yields an equivalent hydraulic conductivity (sometimes termed an "equivalent permeability"). The equivalent hydraulic conductivity of the Hele–Shaw cell is computed as [21]:

$$K_f = \frac{a^2 g}{12 v} \quad (1)$$

where a is the plate spacing and v is the kinematic viscosity of the working fluid (i.e., motor oil). The laminar regime is maintained for Reynolds numbers typically in the 1–10 range for this configuration.

Applicability and Limitations of the Hele–Shaw Analogy

The analogy used here relies on the formal similarity between Darcy's law for saturated seepage in a homogeneous porous medium and the depth-averaged viscous-flow equation between closely spaced parallel plates. Accordingly, the Hele–Shaw cell is appropriate for studying relative changes in hydraulic response caused by blanket length, cutoff depth, and foundation thickness under laminar, steady, two-dimensional conditions. The analogy is not exact: the model does not reproduce soil fabric, pore-scale tortuosity, anisotropy, compressibility, particle detachment, or fluid–solid deformation within the foundation. In addition, the visible interface in the cell is oil-free and air-free. It is therefore a hydraulic analog to the saturated seepage surface, but it is not identical to the infiltration line in a real soil where a negative pressure/unsaturated zone may exist above the phreatic surface. For these reasons, the present measurements are interpreted as relative hydraulic indicators that support preliminary comparison of seepage-control layouts, not as a complete representation of field-scale piping resistance or three-dimensional heterogeneous foundation behavior.

2.3. Experimental Setup (Apparatus, Components, and Flow Circuit)

Experiments were conducted in the Hydraulic Research Laboratory of the Irrigation Engineering and Hydraulics Department, Faculty of Engineering, Alexandria University, Alexandria, Egypt. Figure 2 shows the schematic diagram of the experimental setup. The apparatus comprises two parallel transparent Perspex plates bolted together and mounted vertically in a steel frame. Figure 3 presents a photograph of the laboratory view of the experimental setup. Motor oil is used as the viscous working fluid.

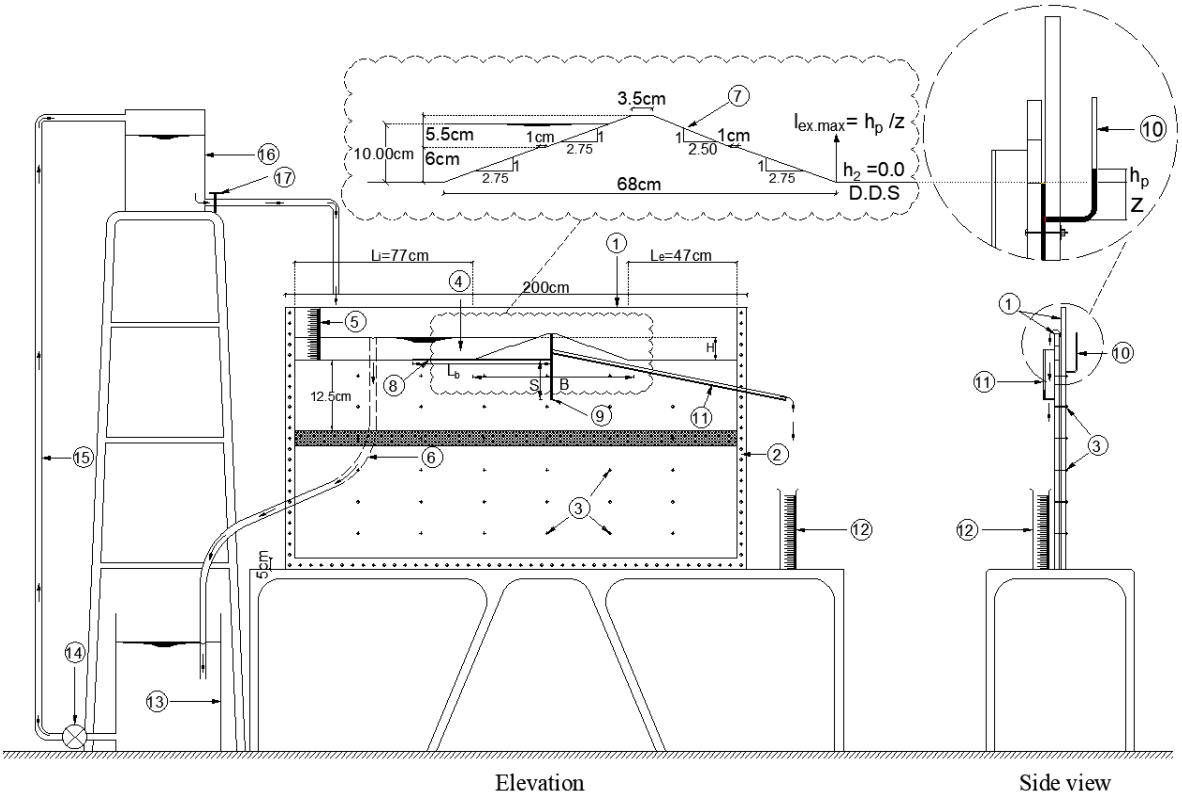

Figure 2. Schematic of the Hele–Shaw setup and instrumentation. (1) Two Perspex plates; (2) klingarite sheet; (3) washers; (4) constant head tank (inflow); (5) vertical scale; (6) overflow tube; (7) dam model; (8) blanket; (9) cut-off; (10) piezometer tube; (11) collecting channel; (12) graduated cylinder; (13) collecting tank; (14) pump; (15) deliver tube; (16) supply tank; (17) control valve.



Figure 3. Photograph of the experimental setup (laboratory view).

2.3.1. Plate Assembly and Spacing Control

- Two Perspex plates (Component 1) with dimensions 2000 mm (length) × 1135 mm (height) × 10 mm (thickness).
- Plate spacing $a = 1.65$ mm maintained by a klingarite sheet band (Component 2) of thickness 1.65 mm and width 50 mm along the base and side boundaries.
- Uniformity of the interspace is ensured by inserting klingarite washers (Component 3) with diameter 10 mm and thickness 1.65 mm, distributed over the plate area and fixed by bolts.

2.3.2. Constant-Head Supply and Measurement

- A constant-head inflow tank (Component 4) supplies the upstream boundary condition.
- A vertical scale (Component 5) with 0.5 mm accuracy measures water/oil levels.

- An overflow tube (Component 6) maintains the prescribed upstream head level during tests.

2.3.3. Model Geometry and Seepage-Control Elements

- The Shiwashok dam cross-section (Component 7) is shaped on the front plate at scale 1:200.
- The upstream blanket (Component 8) and vertical cutoff (Component 9) are formed from an impervious klingarite sheet of thickness 1.65 mm.

2.3.4. Exit-Gradient Measurement

- Piezometer tubes (Component 10) are connected to the back plate just beneath the downstream toe at depths, Z = 2.5, 5.0, 7.5, 10.0 cm, to measure the oil head h_p above the seepage exit datum.

2.3.5. Discharge Collection and Recirculation

- Overflow discharge at the downstream exit is captured by a collecting channel (Component 11) and measured using a graduated cylinder (Component 12).
- Oil from the head tank and collecting channel drains to a collecting tank (Component 13), which is then recirculated by a centrifugal pump (Component 14, 1/3 HP) via a delivery tube (Component 15) to an elevated supply tank (Component 16).
- A thermometer is inserted into the oil to record the temperature for viscosity calculation.

2.4. Model Geometry and Tested Configurations

Three configurations were investigated, as illustrated in Figure 4:

1. Reference condition: dam without seepage-control measures (no upstream blanket and no cutoff).
2. Blanket-only condition: an upstream impervious blanket connected to the dam's impervious element; the blanket length L_b was varied.
3. Blanket–cutoff system: a vertical cutoff wall installed at the blanket termination (downstream tip of the upstream blanket, near the dam), penetrating the pervious foundation to a depth S.

The principal dimensionless parameters are T/B, L_b/B, and S/T. The blanket and cutoff were fabricated from impervious klingarite sheets with thickness consistent with the plate spacing. Table 1 summarizes the tested ranges of foundation thickness T, blanket length L_b, and cutoff depth S.

Table 1. Tested parameter ranges and program layout.

Parameter	Symbol	Values Tested
Foundation thickness	T (cm)	12.5, 17, 34, 51, 68
Foundation thickness ratio	T/B	0.18, 0.25, 0.50, 0.75, 1.00
Blanket length	L_b (cm)	34, 51, 68, 85
Blanket length ratio	L_b/B	0.50, 0.75, 1.00, 1.25
Cutoff depth	S (cm)	2.5, 5, 10, 20, 40, 54.4
Cutoff depth ratio	S/T	0.20, 0.40, 0.60, 0.80

Blanket-only tests covered $0.184 \leq T/B \leq 1.00$ with $0.50 \leq L_b/B \leq 1.25$. Blanket–cutoff tests followed two sub-programs: Approach A, fixed $L_b/B = 0.75$ while varying T/B and S/T; and Approach B, fixed $T/B = 1.00$ while varying L_b/B and S/T.

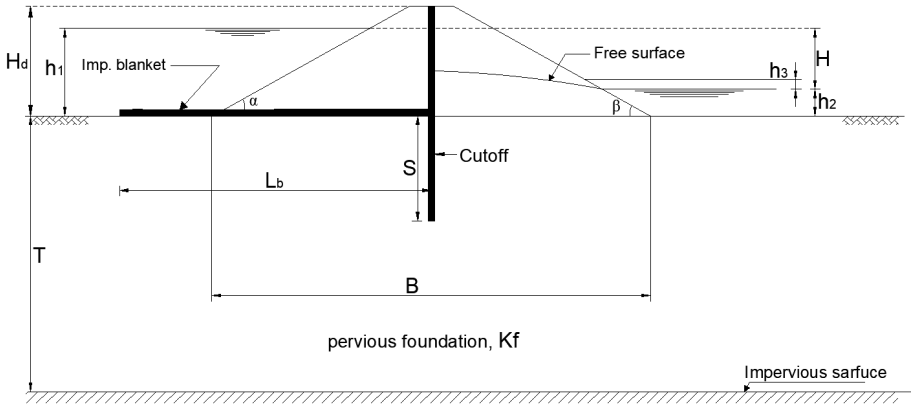

Figure 4. A schematic of the model geometry and parameter definitions (B, H, Hd, L_b, T, S).

2.5. Experimental Procedure and Steady-State Condition

For each tested configuration:

1. The model is assembled for a specified T and seepage-control elements (blanket/cutoff) are installed in accordance with the test case.
2. The upstream head is set to $H = 10$ cm and maintained constant via the overflow tube.
3. Discharge is collected at the downstream outlet in a graduated cylinder at several time intervals.
4. The steady-state condition is assumed when the last two discharge readings are nearly identical.
5. The oil temperature is recorded, viscosity and K_f are computed, and normalized seepage indicators are calculated.

2.6. Measurements

2.6.1. Discharge and Normalized Discharge

After reaching steady state, a volume V collected in time t is used to compute discharge per unit thickness:

$$q = \frac{V}{t} \tag{2}$$

In the Hele–Shaw context, discharge is treated as a per-unit out-of-plane width, yielding units of cm^2/s. The normalized discharge is:

$$\text{Normalized discharge} = \frac{q}{K_f H} \tag{3}$$

2.6.2. Phreatic Line and Downstream Seepage Face Intercept

The phreatic line (seepage-free surface) was traced from the observed interface in the Hele–Shaw cell. The vertical projection of the seepage surface on the downstream face is denoted by h_3, and is normalized by H as h_3/H. In the context of the analog model, this traced line represents the saturated seepage surface in the cell and not the full unsaturated infiltration profile of a real soil mass.

2.6.3. Head Loss Due to Seepage-Control System

Head loss ΔH across the upstream seepage-control layout is measured from the head readings along the upstream control reach and expressed in the normalized form $\Delta H/H$.

2.6.4. Exit Gradient at Downstream Toe

Pressure head readings were taken at downstream toe piezometer points at depths:

$$Z = 2.5, 5, 7.5, 10 \text{ cm}$$

The exit gradient at each depth is:

$$I_{ex} = \frac{h_p}{Z} \tag{4}$$

where h_p is the oil head above the downstream exit datum.

The maximum exit gradient $I_{ex,\max}$ at the ground surface was obtained by extrapolating the $I_{ex} - Z$ relationship to $Z = 0$ at the dam toe, just at the dam toe (Figure 5). Exit gradient results are also reported in the dimensionless product $I_{ex,\max}\,(B/H)$.

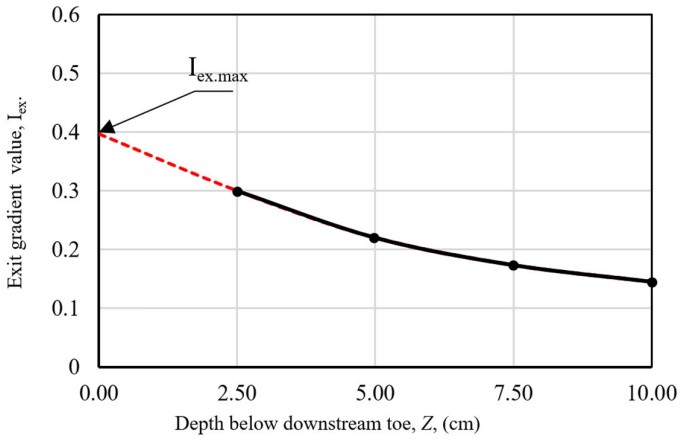

Figure 5. Determination of maximum exit gradient $I_{ex,\max}$ by extrapolation of $I_{ex} = h_p/Z$ versus depth Z to $Z = 0$ at the dam toe.

2.7. Dimensionless Representation

Using Buckingham theory (π-theory), the seepage characteristics were represented using the dimensionless groups:

- $q/(K_f H)$
- $\Delta H/H$
- $I_{ex,\max}(B/H)$
- h_3/H

This form facilitates comparison across runs where oil temperature (and hence K_f) may vary.

2.8. Uncertainty and Quality Control

The following uncertainty-relevant aspects were explicitly considered during the experiments. The vertical measuring scale had an accuracy of 0.5 mm, affecting free-surface readings and therefore h_3, ΔH, and the inferred exit gradients. Steady-state verification was performed by repeated discharge readings until the final two readings were nearly identical, reducing the influence of transient effects on q. Selected configurations were repeated under identical boundary conditions to evaluate experimental repeatability. The variation between repeated runs was within $\pm 3\%$ for the normalized discharge $q/(K_f H)$ and $\pm 5\%$ for the exit-gradient indicator $I_{ex,\max}(B/H)$.

The equivalent hydraulic conductivity K_f depends on the oil viscosity ν, which was evaluated from the measured oil temperature C using [23]:

$$\nu = 23.7316\, e^{-0.064466C} \quad (5)$$

Uncertainty propagation into the principal dimensionless groups can be described by first-order analysis. For $\Pi q = q/\left(K_f H\right)$, the relative uncertainty may be approximated as $\delta\Pi q/\Pi q \approx \left[(\delta q/q)^2 + \left(\delta K_f/K_f\right)^2 + (\delta H/H)^2\right]^{1/2}$, For $\Pi H = \Delta H/\mathrm{H}$ and $\Pi h = h_3/\mathrm{H}$, the corresponding expressions are $\delta\Pi\Delta H/\Pi\Delta H \approx \left[(\delta\Delta H/\Delta H)^2 + (\delta H/H)^2\right]^{1/2}$ and $\delta\Pi h/\Pi\mathrm{h} \approx \left[(\delta h_3/h_3)^2 + (\delta H/H)^2\right]^{1/2}$, where Π is dimensionless parameter and δ is a measurement error. Because K_f is inversely proportional to ν, any temperature-induced uncertainty in viscosity transfers directly to K_f. Using a head-reading accuracy of ± 0.5 mm and a temperature accuracy of approximately ± 0.5 °C, the resulting uncertainty is only a few percent for $q/(K_f H)$ and $\Delta H/\mathrm{H}$, but becomes more sensitive for h_3/H when the downstream seepage-face intercept is very small. The inferred $I_{ex,\max}$ is additionally affected by the extrapolation to $z = 0$, which is why the reported repeatability band ($\pm 5\%$) is more informative than any single local toe reading.

2.9. Regression Modeling for the Blanket-Only Case

For the blanket-only configuration, the linear regression forms to predict normalized seepage characteristics as functions of T/B and L_b/B. These equations are reproduced in Section 3.3 and are proposed here as compact preliminary-design predictors.

3. Results

3.1. Reference Condition (No Blanket, No Cutoff)

Seepage characteristics were first measured for the dam without any seepage-control measures (reference case), as depicted in Figure 6. The experimental results are listed in Table 2 and summarized graphically in Figure 7.

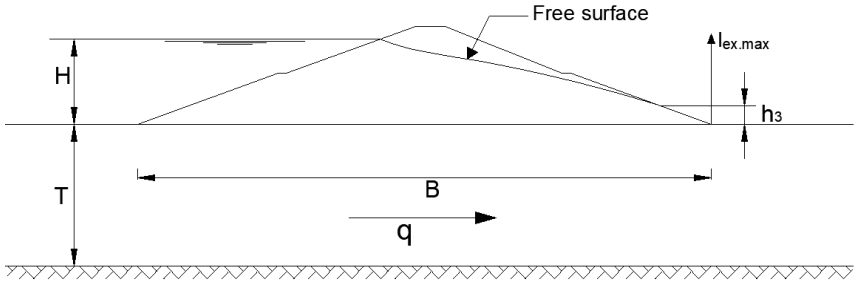

Figure 6. Reference configuration (no seepage-control measures).

Table 2. Reference-case results (no seepage-control measures).

T/B	$q/(K_f H)$	$I_{ex,\max}(B/H)$	h_3/H
0.18	0.3086	2.95	0.236
0.25	0.3646	3.02	0.248
0.5	0.5214	3.19	0.287
0.75	0.6292	3.34	0.311
1	0.7104	3.44	0.328

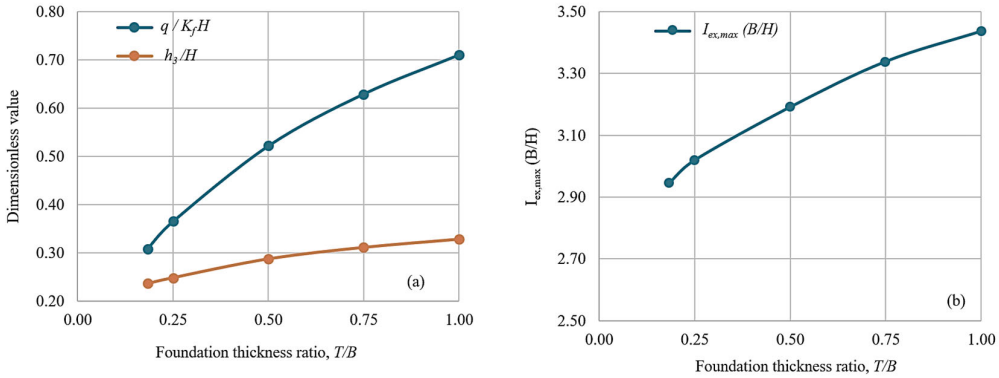

Figure 7. Reference-case seepage response versus foundation thickness ratio T/B: (**a**) normalized discharge $q/(K_f H)$ and downstream seepage-face intercept h_3/H; (**b**) exit-gradient indicator $I_{ex,\max}(B/H)$.

The baseline trends are clear and physically consistent with under-seepage through a pervious foundation layer:

- Discharge increases strongly with foundation depth. As T/B increases from 0.184 to 1.00, the normalized discharge $q/(K_f H)$ increases from 0.3086 to 0.7104 (approximately +130%), reflecting the larger available seepage flow domain and reduced confinement.
- Downstream seepage-face intercept increases with foundation depth. The ratio h_3/H increases from 0.236 to 0.328 (an approximately 39% increase), indicating a higher phreatic surface emerging on the downstream face for thicker pervious layers.
- The exit-gradient indicator increases only moderately. $I_{ex,\max}(B/H)$ rises from 2.95 to 3.44 (a 17% increase). Even though the increase is smaller than that for discharge, it remains relevant for piping sensitivity at the toe.

These results provide the baseline against which blanket-only and blanket–cutoff configurations are evaluated.

3.2. Blanket-Only Configuration (Upstream Impervious Blanket)

Figure 8 illustrates the blanket-only configuration. Experimental results for all combinations of foundation thickness ratio T/B and blanket length ratio L_b/B are listed in Table 3 and plotted in Figure 9.

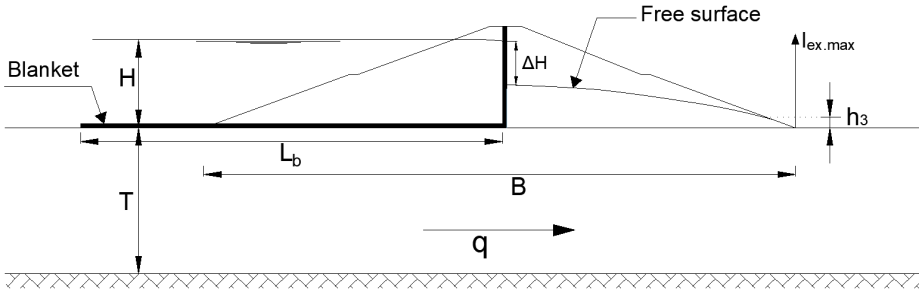

Figure 8. Dam with blanket-only configuration.

For every foundation thickness ratio T/B, increasing L_b/B produces consistent improvements:

- Seepage discharge decreases: $q/(K_f H)$ decreases monotonically with L_b/B. Example at $T/B = 0.50$: $q/(K_f H)$ decreases from 0.36 at $L_b/B = 0.50$ to 0.22 at $L_b/B = 1.25$, which is a substantial improvement.
- Exit-gradient indicator decreases: $I_{ex,\max}(B/H)$ decreases with increasing L_b/B, reflecting reduced toe gradients and improved piping margin.

- Downstream seepage-face intercept decreases strongly: h_3/H decreases sharply as the blanket lengthens, indicating a marked drawdown of the phreatic surface on the downstream slope.
- Head loss across the upstream control system increases: $\Delta H/H$ increases with L_b/B, consistent with the blanket forcing more of the total head loss to occur upstream, thereby lowering gradients near the exit, as desired.

Table 3. Blanket-only results (dimensionless form).

T/B	L_b/B	$q/(K_fH)$	$\Delta H/H$	$I_{ex,\max}(B/H)$	h_3/H
0.18	0.5	0.17	0.57	2.35	0.068
0.18	0.75	0.13	0.61	1.94	0.051
0.18	1	0.11	0.65	1.64	0.034
0.18	1.25	0.09	0.69	1.47	0.017
0.25	0.5	0.22	0.58	2.47	0.075
0.25	0.75	0.17	0.62	2.11	0.058
0.25	1	0.14	0.66	1.83	0.041
0.25	1.25	0.12	0.69	1.6	0.022
0.5	0.5	0.36	0.6	2.94	0.109
0.5	0.75	0.3	0.64	2.7	0.096
0.5	1	0.25	0.67	2.4	0.075
0.5	1.25	0.22	0.7	2.11	0.055
0.75	0.5	0.48	0.63	3.11	0.125
0.75	0.75	0.41	0.66	2.89	0.111
0.75	1	0.35	0.68	2.576	0.091
0.75	1.25	0.31	0.71	2.35	0.066
1	0.5	0.56	0.65	3.22	0.135
1	0.75	0.48	0.68	2.99	0.118
1	1	0.43	0.7	2.7	0.096
1	1.25	0.38	0.71	2.47	0.075

Classical analytical solutions for blanket-only systems predict a monotonic decrease in seepage discharge as blanket length increases [15–18]. The present data show the same functional behavior for every tested T/B: the discharge ratio q/q_0 decreases from about 0.54–0.79 at $L_b/B = 0.50$ to about 0.30–0.53 at $L_b/B = 1.25$, and the curves flatten toward the upper end of the tested range, indicating diminishing marginal benefit. A strict one-to-one numerical benchmark was not attempted because the classical solutions assume idealized Darcy seepage domains and boundary conditions that differ from the present Hele–Shaw analog and zoned-dam geometry. Nevertheless, the agreement in trend and in the observed diminishing-return behavior supports the physical consistency of the experiments.

Although longer blankets always improve performance within the tested range, the incremental improvement generally becomes smaller as L_b/B increases beyond about 1.0. This is especially evident in the percentage-reduction trends in Table 4.

For a fixed blanket length ratio:

- Discharge increases with T/B; thicker pervious layers allow more seepage even with the same blanket geometry.
- The exit-gradient indicator tends to increase with T/B, indicating that deeper foundations remain more challenging and may require either a longer blanket and/or a cutoff to achieve similar gradient reduction.
- Seepage-face intercept increases with T/B, again reflecting the stronger influence of a deeper pervious domain.

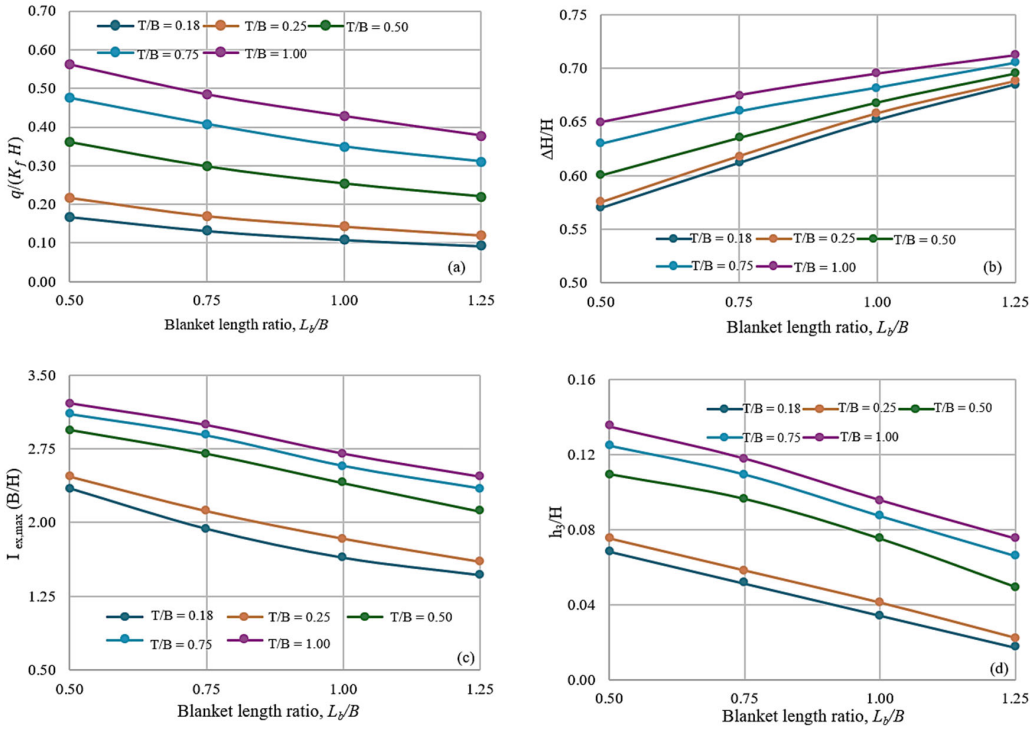

Figure 9. Effect of blanket length ratio L_b/B on seepage indicators for different foundation thickness ratios T/B: (**a**) normalized discharge $q/(K_f H)$; (**b**) head-loss ratio $\Delta H/H$; (**c**) exit-gradient indicator $I_{ex,\max}(B/H)$; (**d**) downstream seepage-face intercept h_3/H.

Table 4. Blanket-only percentage reductions relative to the reference case.

T/B	L_b/B	Δq vs. *ref* (%)	$\Delta I_{ex,\max}$ vs. *ref* (%)	Δh_3 vs. *ref* (%)
0.184	0.5	45.82	20.29	71.01
0.184	0.75	57.49	34.24	78.26
0.184	1	64.98	44.2	85.51
0.184	1.25	70.18	50.18	92.75
0.25	0.5	40.38	18.35	69.66
0.25	0.75	53.37	30.01	76.55
0.25	1	60.82	39.34	83.45
0.25	1.25	67.03	47.12	91.03
0.5	0.5	30.79	7.81	61.9
0.5	0.75	42.8	15.38	66.48
0.5	1	51.24	24.77	73.81
0.5	1.25	57.6	33.83	82.74
0.75	0.5	24.32	6.93	59.84
0.75	0.75	35.14	13.49	64.83
0.75	1	44.44	22.84	71.99
0.75	1.25	50.6	29.72	78.85
1	0.5	20.81	6.4	58.85
1	0.75	31.78	12.9	64.07
1	1	39.72	21.43	70.84
1	1.25	46.81	28.27	77.08

To quantify improvement relative to the reference condition, the percentage reduction (or deviation) is computed as:

$$\Delta y\% = \frac{y_o - y_i}{y_o} * 100, \quad (6)$$

where y_0 is the reference-case value and y_i is the value for the case with a blanket (or blanket–cutoff).

Key findings (blanket-only):

1. Relative to the baseline, the percentage reductions in Table 4 show that the upstream blanket provides substantial seepage-control improvement over the tested parameter range. The normalized discharge decreased by 20.8–70.2%, the exit-gradient indicator decreased by 6.4–50.2%, and the downstream seepage-face intercept decreased by 58.9–92.8%. These ranges indicate that the blanket is most effective at reducing discharge and phreatic emergence, whereas the reduction in exit gradient depends more on foundation thickness and blanket length.
2. The largest reductions occur for shallow foundations (small T/B) and long blankets (large L_b/B).
3. For deep foundations, the blanket remains effective for discharge and phreatic drawdown, but exit-gradient reduction is modest for short blankets (e.g., only around 6% at $T/B = 1.0$, $L_b/B = 0.5$), indicating that a cutoff (or additional measure) becomes more important when T/B is large.

The blanket length substantially changes the free-surface profile compared with the no-blanket case. Figure 10 (shown for $T/B = 0.5$) illustrates the progressive drawdown of the phreatic line as L_b/B increases. For this case, the reduction in the maximum height of the free surface is approximately 45% for $L_b/B = 0.50$ and 60% for $L_b/B = 1.25$ relative to the reference condition.

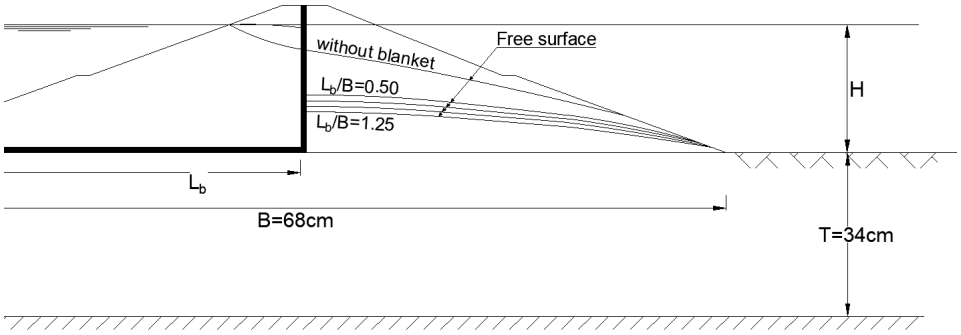

Figure 10. Phreatic line (free-surface) profiles showing the effect of blanket length for a representative case $T/B = 0.25$: comparison between the reference case (no blanket) and blanket-only cases with $L_b/B = 0.50$–1.25.

3.3. Blanket-Only Prediction Equations

For the blanket-only dataset (Table 3), multiple linear regression provides compact predictors (useful for preliminary screening) within the tested ranges:

$$q/\left(K_f H\right) = 0.2121 + 0.4217(T/B) - 0.1745(L_b/B), \quad \left(\mathrm{R}^2 = 0.984\right) \tag{7}$$

$$\Delta H/H = 0.51175 + 0.06649(T/B) + 0.12188(L_b/B), \quad \left(\mathrm{R}^2 = 0.96\right) \tag{8}$$

$$I_{ex,max}(B/H) = 2.664 + 1.217(T/B) - 1.067(L_b/B), \quad \left(\mathrm{R}^2 = 0.96\right) \tag{9}$$

To strengthen confidence in the regression equations, additional validation metrics were computed. Table 5 reports the coefficient of determination, adjusted R^2, RMSE, MAE, and leave-one-out predicted R^2 for the blanket-only models. The results confirm good screening-level predictive performance within the experimental domain, while also indicating that the equations should not be extrapolated beyond the tested ranges.

Table 5. Additional validation metrics for the blanket-only regression equations.

Response	R^2	Adjusted R^2	RMSE	MAE	Predicted R^2 (LOOCV)
$q/(K_f H)$	0.979	0.976	0.020	0.017	0.968
$\Delta H/H$	0.955	0.950	0.009	0.007	0.928
$I_{ex,\max}(B/H)$	0.941	0.934	0.122	0.107	0.920

These equations and metrics should be used only within the tested ranges and as screening tools, whereas final design should rely on detailed seepage analysis and appropriate safety checks.

3.4. Blanket–Cutoff System (Approach A: Fixed L_b/B = 0.75)

To increase control effectiveness, particularly for deeper pervious foundations, a vertical cutoff was added at the blanket termination (Figure 11). In Approach A, the blanket length ratio was fixed at $L_b/B = 0.75$ and the effects of the foundation thickness ratio T/B and cutoff depth ratio S/T were examined. The resulting seepage characteristics are summarized in Table 6.

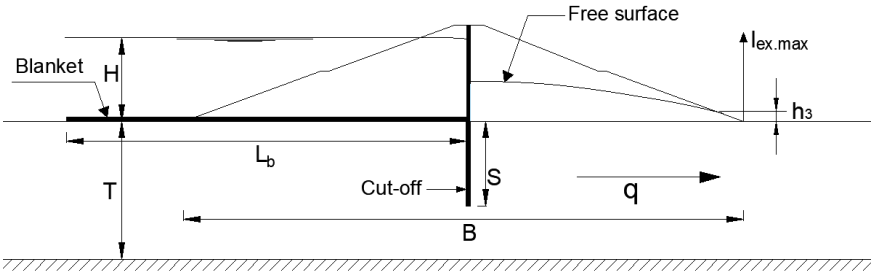

Figure 11. Dam with blanket–cutoff configuration.

Table 6. Blanket–cutoff results for fixed $L_b/B = 0.75$ (dimensionless form).

T/B	*S/T*	$q/(K_f H)$	$\Delta H/H$	$I_{ex,\max}(B/H)$	h_3/H
0.18	0.2	0.129	0.62	1.89	0.048
0.18	0.4	0.125	0.64	1.87	0.041
0.18	0.6	0.119	0.65	1.81	0.033
0.18	0.8	0.111	0.67	1.73	0.024
0.25	0.2	0.168	0.64	2.01	0.053
0.25	0.4	0.162	0.65	1.97	0.045
0.25	0.6	0.153	0.67	1.9	0.037
0.25	0.8	0.141	0.69	1.81	0.027
0.5	0.2	0.293	0.66	2.39	0.086
0.5	0.4	0.278	0.68	2.29	0.073
0.5	0.6	0.256	0.7	2.15	0.058
0.5	0.8	0.226	0.73	1.98	0.044
0.75	0.2	0.392	0.7	2.51	0.098
0.75	0.4	0.367	0.72	2.39	0.082
0.75	0.6	0.33	0.74	2.23	0.066
0.75	0.8	0.281	0.77	2.05	0.05
1	0.2	0.473	0.72	2.57	0.111
1	0.4	0.434	0.74	2.45	0.092
1	0.6	0.385	0.77	2.27	0.074
1	0.8	0.315	0.8	2.1	0.055

3.4.1. Effect of Cutoff Depth S/T on Seepage Indicators

For all tested foundation thickness ratios T/B, increasing the cutoff depth ratio S/T consistently:

- reduces normalized discharge $q/(K_f H)$;

- reduces $I_{ex,\max}(B/H)$;
- reduces h_3/H;
- increases $\Delta H/H$ (i.e., more head dissipation occurs upstream).

These trends are physically consistent with the cutoff forcing the flow path deeper and longer, increasing head loss in the upstream control reach, and reducing gradients at the downstream toe.

The magnitude of improvement with S/T depends strongly on T/B. For example, at a deep foundation with $T/B = 1.00$, increasing S/T from 0.20 to 0.80 reduces $q/(K_f H)$ from 0.473 to 0.315 (≈33% reduction relative to the $S/T = 0.20$ case), reduces $I_{ex,\max}(B/H)$ from 2.57 to 2.10 (≈18% reduction), and reduces h_3/H from 0.111 to 0.055 (≈50% reduction), while increasing $\Delta H/H$ from 0.72 to 0.80 (≈11% increase). In contrast, for a shallow foundation with $T/B = 0.184$, increasing S/T from 0.20 to 0.80 reduces $q/(K_f H)$ from 0.129 to 0.111 (≈14% reduction), reduces $I_{ex,\max}(B/H)$ from 1.89 to 1.73 (≈8% reduction), and also strongly reduces h_3/H from 0.048 to 0.024.

3.4.2. Phreatic Line Response

Figure 12 illustrates the influence of cutoff depth on the observed free surface for a representative case ($T = 34$ cm and $L_b = 51$ cm). Increasing S/T lowers the free surface behind the cutoff, indicating that the barrier promotes upstream head dissipation and suppresses downstream emergence. Relative to the reference case shown in the same figure, the lowering "just behind the cutoff" is approximately 10% at $S/T = 0.20$ and about 30% at $S/T = 0.80$.

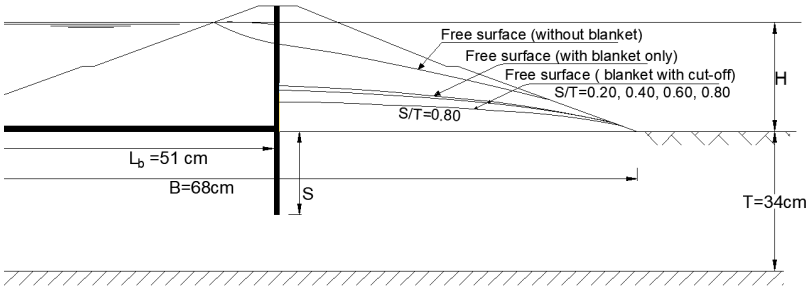

Figure 12. Effect of cutoff depth ratio S/T on the phreatic surface.

3.4.3. Incremental Benefit of Adding the Cutoff over Blanket-Only Performance

To isolate the added value of the cutoff beyond the blanket-only configuration at the same T/B and $L_b/B = 0.75$, the incremental benefit was quantified as:

$$R_{cb,\mathrm{q}}\% = \frac{q_b - q_{cb}}{y_b} * 100 \quad (10)$$

$$R_{cb,\mathrm{I}}\% = \frac{I_{cb} - I_b}{I_b} * 100 \quad (11)$$

where subscript b denotes the blanket-only case and cb denotes the blanket–cutoff case. For head loss, the cutoff contribution is more clearly expressed as an increase relative to the blanket-only condition.

Figures 13 and 14 show the incremental effect of S/T on the discharge and exit-gradient indicators relative to the corresponding blanket-only case. Within the tested range, adding the cutoff produced additional discharge reductions of approximately 0.8–34.4% and additional exit-gradient indicator reductions of approximately 2.6–29.8% relative to blanket-only performance at $L_b/B = 0.75$. The additional reduction in h_3/H reached approximately

55% for the deepest cutoffs. The incremental benefit becomes most pronounced for larger T/B and larger S/T.

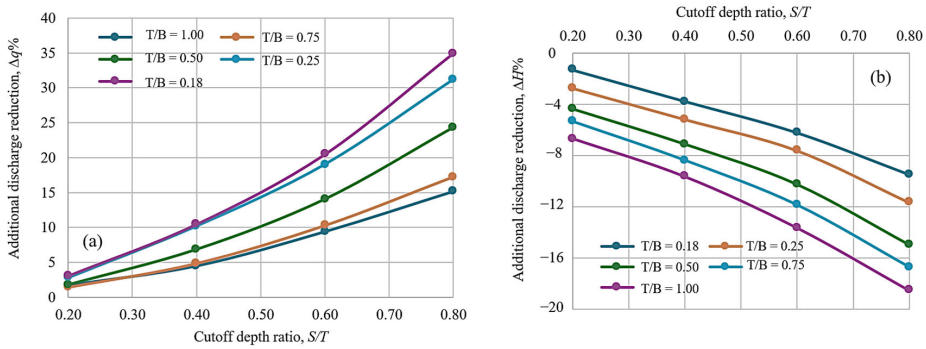

Figure 13. Incremental effect of cutoff depth (fixed $L_b/B = 0.75$) on (**a**) discharge and (**b**) head loss: percentage change relative to the corresponding blanket-only case at the same T/B, plotted versus S/T for $T/B = 0.18$–1.00.

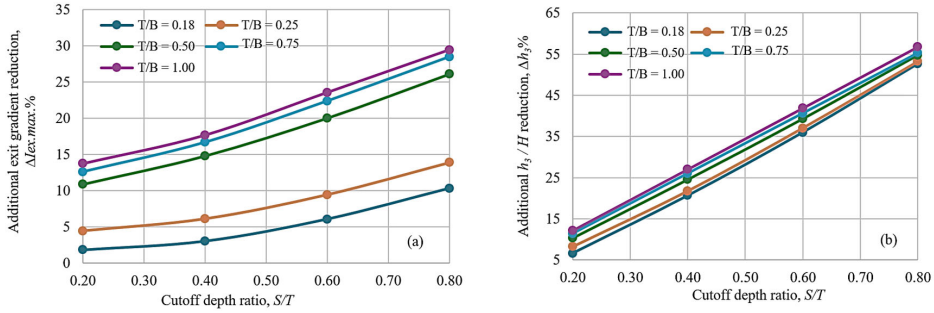

Figure 14. Incremental effect of cutoff depth (fixed $L_b/B = 0.75$) on (**a**) exit-gradient indicator and (**b**) seepage-face intercept: percentage reduction relative to the corresponding blanket-only case at the same T/B, plotted versus S/T for $T/B = 0.18$–1.00.

For design screening, Figure 15 provides a compact map of the incremental benefit of adding the cutoff over the corresponding blanket-only case at $L_b/B = 0.75$, quantified by $R_{cb,q}$ and $R_{cb,I}$. The map highlights where deeper cutoffs provide the greatest additional reductions in discharge and exit-gradient indicator, particularly for larger foundation thickness ratios.

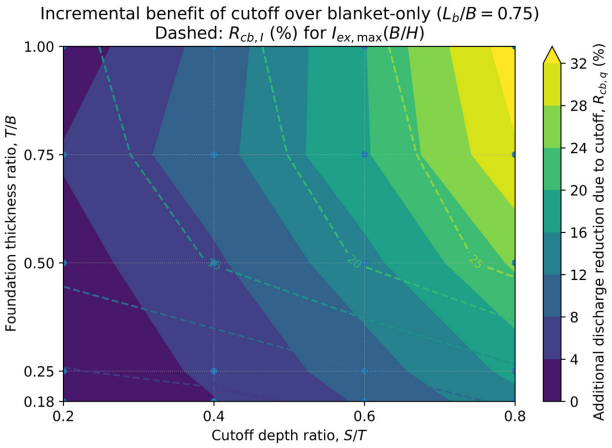

Figure 15. Incremental benefit of adding a cutoff over the blanket-only system $(L_b/B = 0.75)$: filled contours show additional discharge reduction $R_{cb,q}(\%)$ relative to blanket-only, and dashed contours show additional reduction in the exit-gradient indicator $R_{cb,I}(\%)$ relative to blanket-only, both plotted in the T/B–S/T plane. The incremental reductions are computed as $R_{cb,q}(\%) = (q_b - q_{cb})/q_b \times 100$ and $R_{cb,I}(\%) = (I_b - I_{cb})/I_b \times 100$.

3.5. Blanket–Cutoff System (Approach B: Fixed T/B = 1.00)

The combined influence of L_b/B and S/T at the thickest foundation ratio can be examined from the results for $T/B = 1.00$ reported in Table 7.

At fixed $T/B = 1.00$, increasing either blanket length L_b/B or cutoff depth S/T generally improves seepage performance: discharge and the exit-gradient indicator decrease, while $\Delta H/H$ increases.

Cutoff effectiveness depends on blanket length. Figures 16 and 17 (percentage changes compared with blanket-only at the same L_b/B) show that the cutoff provides the largest incremental benefit for shorter blankets. For example, at $L_b/B = 0.50$, deepening the cutoff to $S/T = 0.80$ produces a strong additional reduction in discharge and exit-gradient indicator relative to blanket-only.

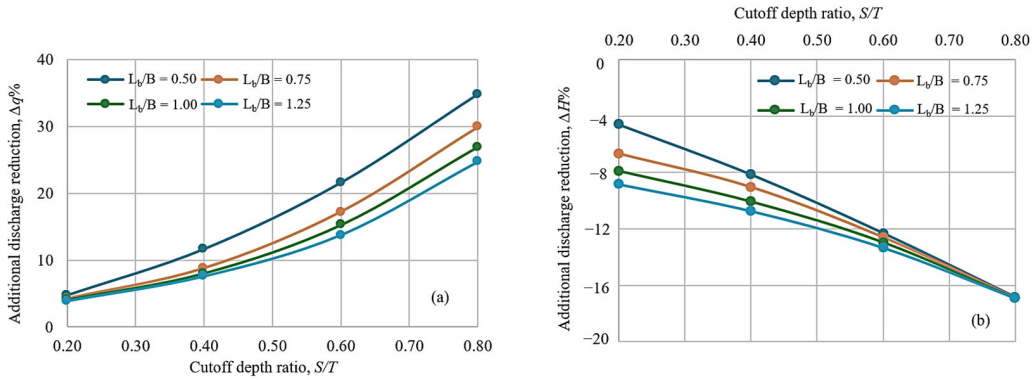

Figure 16. Incremental effect of cutoff depth in a deep foundation ($T/B = 1.00$) on (**a**) discharge and (**b**) head loss: percentage change relative to the blanket-only case at the same L_b/B, plotted versus S/T for $L_b/B = 0.50$–1.25.

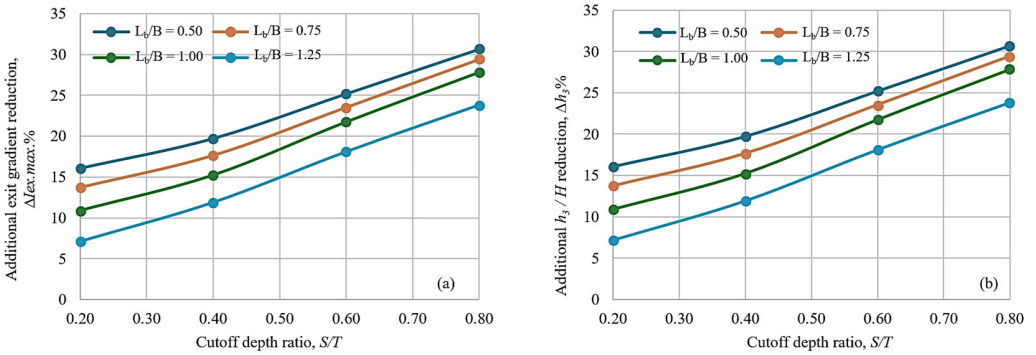

Figure 17. Incremental effect of cutoff depth in a deep foundation ($T/B = 1.00$) on (**a**) exit-gradient indicator and (**b**) seepage-face intercept: percentage reduction relative to the blanket-only case at the same L_b/B, plotted versus S/T for $L_b/B = 0.50$–1.25.

An important nuance for h_3/H is that for the deepest foundation $T/B = 1.00$, a shallow cutoff ($S/T = 0.20$) combined with an already long blanket ($L_b/B \geq 1.00$) produces a slight increase in h_3/H compared with blanket-only in Table 7 (e.g., $h_3/H = 0.103$ vs. 0.086 at $L_b/B = 1.0$). This appears to reflect a redistribution of the flow field/phreatic shape for a shallow barrier placed far upstream. However, deeper cutoffs ($S/T \geq 0.40$) restore the expected trend and reduce h_3/H.

Table 7. Blanket–cutoff results for fixed $T/B = 1.00$ (dimensionless form).

L_b/B	S/T	$q/(K_fH)$	$\Delta H/H$	$I_{ex,\max}(B/H)$	h_3/H
0.5	0.2	0.505	0.68	2.68	0.12
0.5	0.4	0.462	0.703	2.57	0.099
0.5	0.6	0.408	0.73	2.39	0.08
0.5	0.8	0.317	0.759	2.22	0.06
0.75	0.2	0.47	0.72	2.57	0.111
0.75	0.4	0.434	0.736	2.45	0.092
0.75	0.6	0.385	0.76	2.27	0.074
0.75	0.8	0.299	0.789	2.1	0.055
1	0.2	0.427	0.75	2.39	0.103
1	0.4	0.387	0.765	2.27	0.086
1	0.6	0.339	0.785	2.1	0.068
1	0.8	0.267	0.812	1.94	0.051
1.25	0.2	0.376	0.775	2.27	0.086
1.25	0.4	0.339	0.788	2.16	0.072
1.25	0.6	0.299	0.807	2.01	0.059
1.25	0.8	0.242	0.833	1.87	0.044

4. Discussion

4.1. Mechanistic Interpretation (Blanket and Cutoff Effects)

The upstream blanket and cutoff reduce seepage and exit gradient primarily by extending the effective seepage path and redistributing head loss. In continuum terms, the blanket lengthens the portion of the foundation over which potential is dissipated and moves the controlling equipotential drop upstream. The cutoff intensifies this effect by forcing flow beneath the cutoff tip, increasing path length and head dissipation before seepage re-emerges at the downstream side. The measured increases in $\Delta H/H$ together with decreases in $q/(K_fH)$, $I_{ex,\max}(B/H)$, and h_3/H are therefore internally consistent manifestations of the same hydraulic mechanism.

In the blanket-only case, increasing L_b/B increases the distance over which head is dissipated and pulls the phreatic line downward (Figures 9 and 10). Adding a cutoff intensifies this effect by forcing flow beneath the cutoff tip, increasing path length and head dissipation before seepage emerges at the downstream exit (Figures 11–14).

4.2. Context Within Recent Seepage-Control Literature

The direction of improvement observed in this physical modeling study is consistent with recent numerical and case-study research. Combined control measures, such as cutoffs used with drainage, have been shown to reduce seepage risk indicators in parametric and case investigations [4,5], consistent with the additional reductions obtained here when adding a cutoff to a blanket. Seepage-control devices such as drainpipes can reduce seepage and exit gradients while improving stability indices [6], and sheet-pile arrangements similarly modify seepage paths and phreatic profiles [7].

Recent mechanistic work on nonlinear seepage and fluid-solid coupling further indicates that real foundations may depart from linear Darcy-type behavior when deformation and evolving porosity become important [13]. Likewise, probabilistic analyses of layered systems show that spatial variability and stratification can alter reliability metrics and the governing failure mechanism [14]. The present study does not attempt to reproduce those processes; instead, it isolates the hydraulic effect of geometry in a controlled analog experiment. This distinction is important when comparing the present laboratory trends with more comprehensive hydro-mechanical or probabilistic analyses.

The consistency discussed above should be interpreted as qualitative validation of the governing hydraulic trends rather than strict quantitative validation against FEM or prototype measurements. Achieving a quantitative benchmark would require a dedicated numerical model that reproduces the exact Hele–Shaw cell geometry, viscous-fluid properties, boundary conditions, and measurement definitions used in the experiments. That exercise is beyond the present scope. In practice, the present results complement FEM by providing physically measured trend information and screening-level performance maps, whereas FEM remains the appropriate tool for quantitative, site-specific prediction in heterogeneous, anisotropic, or three-dimensional foundations.

4.3. Design Implications and Cost-Effective Ranges

The experimental dataset provides practical guidance for preliminary sizing of seepage-control systems in earth dams founded on pervious strata. In particular, the results allow blanket length and cutoff depth to be linked directly to two hydraulic performance objectives: discharge reduction and exit-gradient reduction.

Figure 18 condenses the blanket-only results in a design-oriented map, showing discharge reduction $R_{b,q}$ as filled contours and exit-gradient indicator reduction $R_{b,I}$ as dashed contours in the $(T/B, L_b/B)$ plane. This representation enables rapid preliminary sizing by selecting a blanket length ratio L_b/B that satisfies both a target discharge reduction and a target reduction in the exit-gradient indicator for a given foundation thickness ratio T/B.

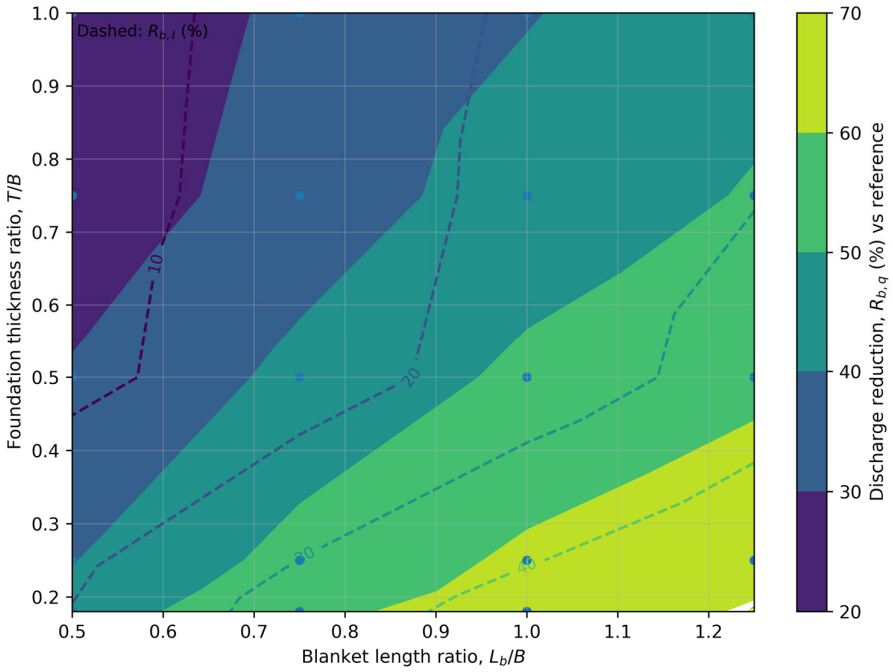

Figure 18. Blanket-only design map from Hele–Shaw experiments: discharge reduction $R_{b,q}$(%) relative to the reference case shown as filled contours in the T/B–L_b/B plane, with exit-gradient indicator reduction $R_{b,I}$(%) shown as dashed contours. Reductions are computed as $R_{b,y}(\%) = (y_0 - y_b)/y_0 \times 100$, where y_0 is the reference-case value and y_b is the blanket-only value at the same T/B.

Relative to current design practice, the dataset contributes a directly measured screening layer between classical closed-form solutions and full numerical analysis. A designer can use Figures 15 and 18 and Equations (7)–(9) to rank blanket/cutoff options rapidly, identify whether a cutoff is likely to provide worthwhile incremental benefit, and then carry only the most promising configurations into detailed seepage, filter, and stability checks.

This is the main practical contribution beyond existing analytical or FEM studies: the paper supplies physically measured relative benefits for coupled design variables rather than only a computed solution for one assumed model form. Within the literature reviewed here, this unified combination of blanket-only and blanket–cutoff cases under one analog framework and one response set is what differentiates the present dataset most clearly from prior experimental and numerical studies.

Based on Figures 9 and 10, Table 4, and the cutoff trends presented in Section 3.4 (including Figure 15), the following design implications are supported within the tested ranges:

- Blanket length selection (L_b/B). Increasing L_b/B consistently reduces $q/(K_f H)$, $I_{ex,\max}(B/H)$, and h_3/H, but the incremental benefit tends to diminish toward the upper end of the tested range. For preliminary screening, $L_b/B \approx 0.75$ provides a practical baseline because it yields substantial reductions across all tested T/B values.
- Conditions under which a cutoff is most beneficial. For deeper pervious foundations ($T/B \gtrsim 0.5$), the blanket-only exit-gradient reduction can be modest at shorter blanket lengths, and the incremental benefit of adding a cutoff becomes significant. Figure 15 shows that deeper cutoffs ($S/T \approx 0.6$–0.8) provide the largest additional reductions in both discharge and exit-gradient indicator.
- Cutoff depth selection and head-loss tradeoff. Increasing S/T increases $\Delta H/H$, indicating greater head dissipation upstream. This redistribution is favorable for lowering toe gradients, but very deep cutoffs should still be evaluated against construction feasibility and cost.
- Use as screening tools, not final design. Figure 18 and the regression equations in Section 3.3 provide rapid preliminary sizing for blanket-only systems, while Figure 15 provides a concise screening view of the cutoff's incremental value. Final design should still be verified by detailed seepage analysis and appropriate internal erosion control measures, including filters and toe drainage where necessary.

4.4. Interpretation of Exit-Gradient Indicator and 2D–3D Applicability

To relate the exit-gradient indicator to conventional piping interpretation, note that $I_{ex,\max} = [I_{ex,\max}(B/H)]\cdot(H/B)$. For the present prototype geometry, $H/B = 20/136 \approx 0.147$, so the measured indicators correspond to approximate exit gradients of about 0.22–0.51 across the tested cases. These values are below the classical boiling-type critical gradient of order unity for many noncohesive soils, but internal erosion may start at substantially lower local gradients depending on gradation, structure, and filter compatibility [2,3]. Therefore, the reported exit-gradient quantity should be interpreted as a comparative hydraulic index rather than a direct pass/fail piping criterion.

The experiments represent a two-dimensional central cross-section of the dam-foundation system. In a real foundation, three-dimensional flow may develop near abutments, blanket ends, cutoff terminations, drains, and local heterogeneities, which can modify both total seepage and local exit gradients. Accordingly, the present results are most applicable to preliminary screening of long, laterally uniform reaches rather than final design of spatially complex foundations.

4.5. Limitations and Pathways to Extend the Work

This study is limited to a homogeneous pervious foundation, steady upstream head, laminar viscous analog flow, and the tested intervals $0.18 \le T/B \le 1.00$, $0.50 \le L_b/B \le 1.25$, and $0.20 \le S/T \le 0.80$. Extrapolation outside these ranges is not recommended. The Hele–Shaw analogy also excludes spatial variability, anisotropy, soil-structure deformation, particle migration, and long-term material degradation. Future work should examine lay-

ered and anisotropic foundations, transient reservoir operation, filter/drain combinations, and coupled hydraulic-mechanical behavior, preferably in combination with numerical and probabilistic analyses to extend the present dataset toward field conditions.

5. Conclusions

Based on the Hele–Shaw experimental and dimensionless data reduction, the following conclusions are drawn:

1. Baseline sensitivity to foundation thickness (reference condition): Without seepage-control measures, increasing T/B increases $q/(K_f H)$, increases h_3/H, and moderately increases the exit-gradient indicator $I_{ex,\max}(B/H)$ over the tested range $0.184 \leq T/B \leq 1.00$.
2. Blanket-only effectiveness: Relative to the reference case, the upstream impervious blanket reduces seepage discharge, toe exit-gradient indicator, and seepage-face intercept substantially. Overall, after testing T/B and L_b/B, the blanket achieved:
   - Discharge reduction: 20.8–70.2%;
   - Exit-gradient indicator reduction: 6.4–50.2%;
   - Seepage-face intercept reduction: 58.9–92.8%.
3. Influence of blanket length: Increasing L_b/B consistently improves seepage performance (by lowering $q/(K_f H)$, $I_{ex,\max}(B/H)$, and h_3/H) while increasing $\Delta H/H$. The incremental benefit generally diminishes as L_b/B becomes large (beyond about 1.0 in the tested range).
4. Added value of cutoff: Adding a vertical cutoff to the blanket (blanket–cutoff system) produces additional reductions in discharge, exit-gradient indicator, and seepage-face intercept compared with blanket-only performance, particularly for larger S/T and deeper foundations (larger T/B).
5. Head-loss redistribution: The blanket–cutoff system increases $\Delta H/H$, consistent with shifting head dissipation upstream and reducing downstream gradients.
6. Compact prediction tools: Regression equations for the blanket-only case (Equations (7)–(9)) predict $q/(K_f H)$, $\Delta H/H$, and $I_{ex,\max}(B/H)$ as linear functions of T/B and L_b/B, providing a practical preliminary-design screening tool within the tested parameter ranges.
7. These results provide a physical basis for ranking the relative effectiveness of seepage-control measures, but specific design for a real dam foundation must also consider material heterogeneity, unsaturated behavior, construction details, and three-dimensional seepage effects. Agreement with prior analytical and numerical studies should therefore be interpreted as qualitative trend validation, while quantitative site-specific design remains the role of FEM or similarly detailed seepage models.

Author Contributions: Conceptualization, A.M.A., M.A.H. and M.A.A.; methodology, A.M.A., M.A.H. and M.A.A.; investigation, A.M.A., M.A.H. and M.A.A.; formal analysis, A.M.A., M.A.H., M.A.A. and A.M.; data curation, A.M.A., M.A.H., M.A.A. and A.M.; writing—original draft preparation, M.A.H., M.A.A. and A.M.A.; writing—review and editing, A.M.A. and A.M.; supervision, M.A.A. and A.M.A. All authors have read and agreed to the published version of the manuscript.

Funding: This research received no external funding.

Data Availability Statement: All data supporting the reported results are included in the manuscript tables.

Acknowledgments: The authors would like to thank Prince Sultan University for paying the Article Processing Charges (APC) for this publication.

Conflicts of Interest: The authors declare no conflicts of interest.

Nomenclature

The following abbreviations are used in this manuscript:

a	Plate spacing
B	Dam base width
b	Dam crest width
C	Oil temperature
ΔH	Head loss along upstream control system
g	Gravitational acceleration
H	Upstream head
H_d	Dam height
h_3	Vertical projection of seepage surface on downstream face
h_p	Pressure head at a piezometer point
I_{ex}	Exit gradient at depth (Z)
$I_{ex,max}$	Maximum exit gradient at ground surface
K_f	Equivalent Hele–Shaw hydraulic conductivity
L_b	Upstream impervious blanket length
q	Seepage discharge per unit width (per unit out-of-plane thickness)
S	Cutoff depth
T	Pervious foundation thickness
ν	Kinematic viscosity
Z	Piezometer depth below exit point
$R_{b,q}$	Discharge reduction due to blanket relative to reference $[(q_0 - q_b)/q_0] \times 100$
$R_{b,I}$	Exit-gradient indicator reduction due to blanket relative to reference $[(I_0 - I_b)/I_0] \times 100$
$R_{cb,q}$	Additional discharge reduction due to cutoff relative to blanket-only $[(q_b - q_{cb})/q_b] \times 100$
$R_{cb,I}$	Additional exit-gradient indicator reduction due to cutoff relative to blanket-only $[(I_b - I_{cb})/I_b] \times 100$
$q/(K_f H)$	Normalized seepage discharge
$\Delta H/H$	Normalized head-loss ratio
h_3/H	Normalized downstream seepage-face intercept
$I_{ex,\max}(B/H)$	Dimensionless exit-gradient indicator

References

1. EL Molla, D.A.; Kilit, M. Seepage Control, Detection, and Treatment in Embankment Dams: A State-of-the-Art Review. *Arab. J. Sci. Eng.* **2025**, *51*, 3823–3849. [CrossRef]
2. Li, M.; Fannin, R.J. Internal erosion: Critical hydraulic gradient in one-dimensional vertical seepage and its relation to soil gradation. *Can. Geotech. J.* **2022**, *59*, 769–772. [CrossRef]
3. Chen, C.; Zhang, P.; Zhang, L.; Zhang, J.; Xue, J.; Lu, H. Internal erosion in granular soils with different microstructures under cyclically increased hydraulic gradients. *J. Hydrol.* **2024**, *639*, 131601. [CrossRef]
4. Brontowiyono, W.; Hammid, A.T.; Jebur, Y.M.; Al Sudani, A.Q.A.S.; Mutlak, D.A.; Parvan, M. Reduction of Seepage Risks by Investigation into Different Lengths and Positions for Cutoff Wall and Horizontal Drainage (Case Study: Sattarkhan Dam). *Adv. Civ. Eng.* **2022**, *2022*, 6441646. [CrossRef]
5. Charrak, H.; Smail, N.; Rouissat, B. Influence of Combination of the Cutoff Wall and Horizontal Drainage on Seepage Characterization in Earth Dam Foundations. *Indian Geotech. J.* **2023**, *53*, 995–1010. [CrossRef]
6. Hassan, W.H.; Zwain, H.M. The influence of drain pipe location and diameter on seepage through an earth dam. *Ain Shams Eng. J.* **2024**, *15*, 102475. [CrossRef]
7. Haghdoost, M.; Sajjadi, S.M.; Ahadiyan, J.; Norouzi, R.; Abraham, J. The effect of sheet piles' inclination angle, number, and distance on seepage through an earthfill dam. *Ain Shams Eng. J.* **2024**, *15*, 103056. [CrossRef]
8. Wang, T.; Wang, Z.; Li, Y.; Yuan, H.; Chai, J.; Liu, Y. Seepage features and reliability analysis of deep overburden dam foundations considering the spatial variability in permeability. *Comput. Geotech.* **2025**, *183*, 107217. [CrossRef]
9. Pourbeirak, S.; Johari, A.; Daneshvar, F.A.; Habibagahi, G. Reliability analysis of seepage in earth dam considering saturated–unsaturated flow: A case study. *Comput. Geotech.* **2026**, *191*, 107797. [CrossRef]

10. Salman, M.M.; Mohammadi, M.; Shakouri, B. Analysis of the seepage and stability in a non-homogeneous earth dam under transient conditions: A case study. *Ain Shams Eng. J.* **2026**, *17*, 103825. [CrossRef]
11. Guo, C.; Lu, J.; Song, Z.; Li, H.; Zhang, W.; Li, Y. Durability analysis of concrete cutoff wall of earth rock dams considering seepage and dissolution coupling effect. *Water* **2024**, *16*, 1590. [CrossRef]
12. Alrowais, R.; Alwushayh, B.; Bashir, M.T.; Nasef, B.M.; Ghazy, A.; Elkamhawy, E. Modeling and Analysis of Cutoff Wall Performance Beneath Water Structures by Feed-Forward Neural Network (FFNN). *Water* **2023**, *15*, 3870. [CrossRef]
13. Cao, Z.; Xie, M.; Tao, R.; Feng, D.; Li, Z.; Wang, W. Nonlinear Seepage Mechanical Model and Bifurcation Analysis for Fluid–Solid Coupling in Fractured Rock Mass. *Sci. Rep.* **2026**, *16*, 9578. [CrossRef]
14. Zhu, D.; Griffiths, D.V.; Fenton, G.A.; Huang, J. Probabilistic Stability Analyses of Two-Layer Undrained Slopes. *Comput. Geotech.* **2025**, *182*, 107178. [CrossRef]
15. Bennett, P.T. The Effect of Blankets on Seepage through Pervious Foundation. *Trans. Am. Soc. Civ. Eng.* **1946**, *111*, 215–228. [CrossRef]
16. Rezk, M.; Senoon, A. Analytical solution of earth dam with upstream blanket. *Alex. Eng. J.* **2012**, *51*, 45–51. [CrossRef]
17. Ghanbari, A.; Zaryabi, S. A simple method for calculating seepage at the foundation of embankment dams with blanket and clay trench. *J. GeoEng.* **2014**, *9*, 21–32.
18. Salmasi, F.; Noori, M. Effect of upstream semi-impervious blanket of embankment dams on seepage. *ISH J. Hydraul. Eng.* **2019**, *25*, 143–152. [CrossRef]
19. Amer, M.; Abourohiem, M.A.; Abdelrazek, A.M. Influence of Upstream Impervious Blanket with Vertical Cutoff on Seepage through Earth Dam. In Proceedings of the 3rd International Conference of Chemical, Energy and Environmental Engineering, Alexandria, Egypt, 19–21 July 2021; pp. 50–56.
20. Noori, M.; Ibrahim, H.; Hasan, A. Influence of upstream blanket on earth dam seepage. In Proceedings of the 4th International Engineering Conference on Developments in Civil & Computer Engineering Applications, Erbil, Iraq, 26–27 February 2018; pp. 178–188. [CrossRef]
21. Hele Shaw, H.S. Experiments on the nature of the surface resistance in pipes and on ships. *Trans. Inst. Nav. Archit.* **1897**, *39*, 145–156.
22. Stemberg, Y.M.; Scott, V.H. The Hele Shaw model—A Research Device in Ground-Water Studies. *Groundwater* **1964**, *2*, 33–37. [CrossRef]
23. Gobran, A.A. Analysis of a System of Tile Drainage Assisted by Mole Drains. Ph.D. Thesis, Alexandria University, Alexandria, Egypt, 1991.

Disclaimer/Publisher's Note: The statements, opinions and data contained in all publications are solely those of the individual author(s) and contributor(s) and not of MDPI and/or the editor(s). MDPI and/or the editor(s) disclaim responsibility for any injury to people or property resulting from any ideas, methods, instructions or products referred to in the content.